Hydrodesulfurization of dibenzothiophene over Ni–Mo sulfides supported by proton-exchanged siliceous MCM-41

Xiang Li [a], Anjie Wang [a,*], Yao Wang [a], Yongying Chen [a], Yihui Liu [a] and Yongkang Hu [b]

[a] State Key Laboratory of Fine Chemicals, Dalian University of Technology, 158 Zhongshan Road, Dalian 116012, Peoples Republic of China
[b] Fushun Research Institute of Petroleum and Petrochemicals, 31 Dandong Road, Fushun 113001, Peoples Republic of China

Received 25 February 2002; accepted 15 August 2002

Strong acid sites on the surface of mesoporous MCM-41 were generated by ion-exchanging siliceous MCM-41 with dilute HNO_3 solution (0.5 M). The XRF determination indicates that most of the sodium cations contained in MCM-41 can be removed by the proton exchange, and dealuminization was observed during the proton exchange. The acidity of the mesoporous materials was characterized by means of NH_3–TPD and the Hammett indicators. It is revealed that new strong acid sites ($-5.6 > H_0 > -8.2$) were generated after the first 2 h of ion exchange and that the following ion exchanges had little effect on the acidic properties. XRD patterns of the mesoporous materials indicate that the structure of siliceous MCM-41 was improved by HNO_3 ion exchange. When Ni–Mo sulfides were supported on the prepared solid acid (H^+–MCM-41), high performance in the hydrodesulfurization (HDS) of dibenzothiophene (DBT) was observed. However, the HDS activity was decreased while the selectivity of biphenyl (BP) was increased, when H^+–Si–MCM-41 was ion exchanged with Na_2CO_3 aqueous solution. TPR profiles of the supported Ni–Mo oxides reveal that the acidic properties of the supports greatly influence the hydrogenation activities of the bimetallic oxides. The high performance of H^+–MCM-41-supported Ni–Mo catalysts may be attributed to the enhanced hydrogenation activity. The introduction of Na cation into the support led to the decrease of the HDS activity due to the poor hydrogenation ability of the supported bimetallic oxides. The HDS activity is well correlated with the low H_2 consumption temperature in the TPR profiles.

KEY WORDS: siliceous MCM-41; HNO_3 ion exchange; acidity; hydrodesulfurization; dibenzothiophene.

1. Introduction

Mesoporous MCM-41 has been the focus of much research interest since its discovery because it offers a uniform pore of 15 to 100 Å, a very high surface area and mild acidity [1,2]. MCM-41-supported catalysts have been developed for a variety of reactions [3], including hydrodesulfurization (HDS) of petroleum fractions [4–8].

It is interesting to note that most of the research on MCM-41-supported HDS catalysts has focus on Al–MCM-41 [4–8], probably hoping that the strong acidity of the support may help to crack the polyaromatic sulfur-containing compounds so as to improve the HDS activity. Nevertheless, no great improvement in HDS activity has been achieved. In contrast to Al–MCM-41, siliceous MCM-41 (Si–MCM-41) is structurally stable to thermal treatment up to 700 °C, hydrothermal treatment with steam at mild conditions, mechanical grinding and acid treatment at mild conditions [9]. It is supposed that the structural Al in Al–MCM-41 renders the mesostructure unstable even to mild thermochemical treatment [10]. Moreover, the incorporation of Al into the Si–MCM-41 framework causes a deterioration of the textural characteristics and some loss in the periodicity of the MCM-41 pore structure [8].

* To whom correspondence should be addressed.
E-mail: anjwang@chem.dlut.edu.cn

Recently, we have investigated the HDS of dibenzothiophene (DBT), a refractory sulfur-containing molecule in petroleum fraction, over Si–MCM-41-supported Co–Mo, Co–W and Ni–W sulfides [11,12]. It is shown that Si–MCM-41-supported catalysts were superior in HDS activity to the conventional alumina-supported ones. It is assumed that the high performance is due to the higher dispersion of the active species on the surface of MCM-41. Nevertheless, since the silica source in synthesizing MCM-41 is sodium silicate hydrate, the sodium cations on the surface of MCM-41 may have influences on the acidic properties of Si–MCM-41 and may affect the HDS activity of supported catalysts.

The objective of this paper is to study the acidic properties of Si–MCM-41 after being ion exchanged with dilute HNO_3 solutions and the performance of its supported Ni–Mo sulfides in HDS of DBT.

2. Experimental

The materials used were sodium silicate hydrate (commercial GR grade), cetyltrimethylammonium bromide (CTAB) (A.R. grade), 4 M H_2SO_4, 0.5 M HNO_3 and 0.25 M Na_2CO_3. Both ammonium heptamolybdate tetrahydrate [$(NH_4)_6Mo_7O_{24}{\cdot}4H_2O$] and nickel nitrate hexahydrate [$Ni(NO_3)_2{\cdot}6H_2O$] were of commercial GR grade (Dalian Chemical Reagents Co.). Dibenzothiophene

1011-372X/02/1100-0107/0

was synthesized according to the method in the literature [13]. Decalin was a product of Shanghai Chemical Reagents Co. and used as solvent without further purification. The Hammett indicators included p-(dimethylamino) azobenzene (pKa = +3.3), dicinnamalacetone (pKa = −3.0), benzalacetophenone (pKa = −5.6), and anthraquinone (pKa = −8.2) [14].

Si–MCM-41 was synthesized using sodium silicate hydrate as the source of SiO_2 and CTAB as the template, following the procedure reported in the previous paper [15]. The proton-exchanged MCM-41 was prepared as follows: 1 g of Si–MCM-41 was added into 10 ml of 0.5 M HNO_3 solution; the mixture was stirred for 2 h at ambient temperature; the mixture was separated by filtration and the solid product was washed with the de-ionized water until the pH of the effluent solution reached 7; then the solid product was dried at 120 °C overnight. When necessary, the above procedure was repeated. Finally, the dried sample was calcined at 540 °C for 3 h to obtain the proton-exchanged MCM-41. The proton-exchanged MCM-41 was denoted as H^+–MCM-41(t), where t represents the total ion-exchange time, *i.e.*, 2 multiplied by the exchange times. To investigate the effect of Na^+, the ion exchange of H^+–MCM-41(6) with 0.25 M of Na_2CO_3 solution was performed in a similar way. The product was denoted as Na–MCM-41.

H^+–MCM-41(t) was characterized by means of N_2 adsorption, XRD, NH_3–TPD and Hammett indicators. The X-ray diffraction (XRD) patterns were recorded on a Rigaku D-Max-2400 diffractometer using Cu K_α radiation at 40 kV and 100 mA. Nitrogen adsorption–desorption was performed using a Quantachrome adsorption analyzer, which reports isotherms and BET specific surface area and pore volume automatically. Before the adsorption analysis, the samples were outgased for 3 h at 300 °C. The NH_3–TPD data were collected using a Chembet 3000 analyzer. About 200 mg sample was activated in flowing He at 500 °C for 2 h, then cooled to 120 °C under continuous evacuation. The sample was equilibrated with gaseous NH_3 at 0.04 kPa, then ramped up at 10 °C min^{-1} while He flows through the reactor at 20 cm^3 min^{-1}. The acidity of H^+–MCM-41(t) was measured by means of the Hammett indicators mentioned above. The samples were pretreated in a muffle furnace at 300 °C for 2 h, prior to acidity measurement. The contents of sodium and aluminum of MCM-41 before and after the ion exchange were determined by means of an XRF analyzer (RSR 3400 X).

Ni–Mo/H^+–MCM-41(t) was prepared in the following way: H^+–MCM-41(t) was impregnated with an aqueous solution of $(NH_4)_6Mo_7O_{24}$ and $Ni(NO_3)_2$ for 8 h at room temperature, then the water was evaporated and the solid product was dried at 120 °C overnight, and calcined at 450 °C for 5 h. A 20 wt% MoO_3 loading level and an Ni/Mo atomic ratio of 0.75 were chosen in this study. For comparison, Na–MCM-41-supported Ni–Mo catalyst was prepared in the same way.

The temperature programmed reduction (TPR) profiles of H^+–MCM-41(t)-supported and Na–MCM-41-supported Ni–Mo catalysts were measured on a Chembet-3000 analyzer. Before the measurement, the samples were treated in argon at 200 °C for 12 h. A gas mixture of H_2 and Ar (5 vol% H_2 in argon) was used as the reacting agent. The TPR profiles of the catalysts were measured from room temperature to 930 °C at 10 °C min^{-1}. For comparison, the profile of an Ni–Mo/γ-Al_2O_3 catalyst was also measured.

HDS of DBT was carried out in a fixed-bed stainless steel tubular reactor having a dimension of 8 mm in internal diameter. 0.2 g of the catalyst was charged. Prior to charge, the catalyst was pelleted and then crushed and screened to 20–35 mesh. The HDS activities of the prepared catalysts were evaluated using a model fuel: 0.8 wt% DBT in decalin.

The catalysts were presulfided before HDS reaction by a mixture of H_2S/H_2 (10 vol% H_2S) at atmospheric pressure and 400 °C for 3 h. The reaction conditions for HDS reaction were temperature 260–340 °C, total pressure 5.0 MPa, H_2/feed ratio 1200 Nm^3 m^{-3}, and WHSV 12 h^{-1}. The products were analyzed by an Agilent-6890$^+$ gas chromatograph equipped with an FID detector using an HP-5 column.

3. Results and discussion

3.1. Characterization of H^+–MCM-41(t)

The XRD patterns of Si–MCM-41 and its proton-exchanged products are shown in figure 1. It can be seen that all the samples show diffraction reflections at *ca* $2\theta = 2°$, suggesting that the mesopore structure undergoes little change during the proton exchange, and the diffraction intensity increases considerably after the siliceous MCM-41 is ion-exchanged for 2 h while little changes are observed in the following ion exchange. However, the diffraction intensity of the mesoporous material decreases considerably after being exchanged for 8 h, indicating that part of the mesostructure may collapse.

The structural parameters characterized by XRD and N_2 adsorption are summarized in table 1. It is shown that the interplanar spacing d_{100} changes from 38.7 to 42.2 Å and the pore size from 24.6 to 27.4 Å, indicating that the mesopores are enlarged after the ion exchange. Accordingly, the surface area, pore volume and relative crystallinity increase remarkably.

Table 2 summarizes the content of sodium and aluminum contained in the Si–MCM-41 and its proton-exchanged products. It is indicated that the sodium can be completely removed by proton exchange, and dealuminization was observed during the proton exchange.

Table 1
Structural parameters of siliceous MCM-41 and its proton-exchanged products.

	Si–MCM-41	H^+–MCM-41(2)	H^+–MCM-41(4)	H^+–MCM-41(6)	H^+–MCM-41(8)
2θ (°)	2.28	2.08	2.02	2.06	2.1
d_{100} (Å)	38.7	42.4	43.7	42.9	42
Relative crytallinity (%)	10	89.6	91	100	16
BET specific area ($m^2\ g^{-1}$)	841.1	849.4	875.1	875.0	893.4
Pore volume change after proton exchange (%)	–	12	0.2	13	13.2
Pore size (BJH) (Å)	24.6	27.4	27.4	27.4	27.4

However, dealuminization was not observed during the ion exchange with Na_2CO_3. The sharp increase of the diffraction intensity may be attributed to the clearing-up of the mesopore channels, as reflected by the improvement of the structural parameters. It should be noted that the weight of the sample changed a little after the ion exchange if the weight loss due to the decrease of the atomic mass of the cations is taken into account. It is assumed that the increase of crystallinity after proton exchange might result partly from the clearing-up of the blocks in the mesopores and partly from the reconstruction of the mesostructure.

The NH_3–TPD profiles of Si–MCM-41 and the proton-exchanged products are shown in figure 2. It can be seen that there is only one peak at low temperature for siliceous MCM-41, whereas a very strong peak at high temperature is observed for the proton-exchanged MCM-41. The appearance of a strong high-temperature peak indicates that new strong acid sites might be generated on the surface after the proton exchange. But it seems that the exchange time has little effect on the acidity of MCM-41 since no significant changes of the peak temperature were observed for H^+–MCM-41(4), H^+–MCM-41(6), and H^+–MCM-41(8).

The strong acidity of H^+–MCM-41 is reconfirmed by the color change method using a Hammett indicator, as shown in table 3. It can be seen that the Hammett acidity of Si–MCM-41 is $+3.3 > H_0 > -3.0$, whereas the acidities of the proton-exchanged MCM-41 are rather stronger ($-5.6 > H_0 > -8.2$). Similarly, little changes in acidity were detected by increasing the ion-exchange time, in accordance with the results of NH_3–TPD.

The results from both NH_3–TPD and Hammett indicators reveal that Si–MCM-41 only possesses some acid sites of weak and middle strength ($+3.3 > H_0 > -3.0$) similar to Al–MCM-41. However, new strong acid sites ($-5.6 > H_0 > -8.2$) were generated after the proton exchange.

Table 2
The contents of sodium and aluminum in MCM-41 before and after the ion exchange.

	Concentration (%)	
	Na_2O	Al_2O_3
Si–MCM-41	1.1	1.4
H^+–MCM-41(2)	n.d.	0.96
H^+–MCM-41(4)	n.d.	0.98
H^+–MCM-41(6)	n.d.	0.75
H^+–MCM-41(8)	n.d.	0.67
Na–MCM-41	1.4	0.75

3.2. Hydrodesulfurization of DBT

A model fuel containing 0.8 wt% DBT in decalin was used to investigate the HDS activities of the supported Ni–Mo catalysts. The main products of HDS of DBT are biphenyl (BP) and cyclohexylbenzene (CHB). The HDS reaction path network of DBT is shown in figure 3 [6]. HDS of DBT mainly takes place in two paths, *i.e.*, HDS *via* C–S bond scission to form BP (hydrogenolysis path) and hydrogenation followed by desulfurization to form CHB (hydrogenation path). Since it is difficult to hydrogenate BP to form CHB, the selectivity of BP (S_{BP}) is usually used to represent the hydrogenolysis path and that of CHB (S_{CHB}) to determine the hydrogenation path. Benzene and cyclohexane are

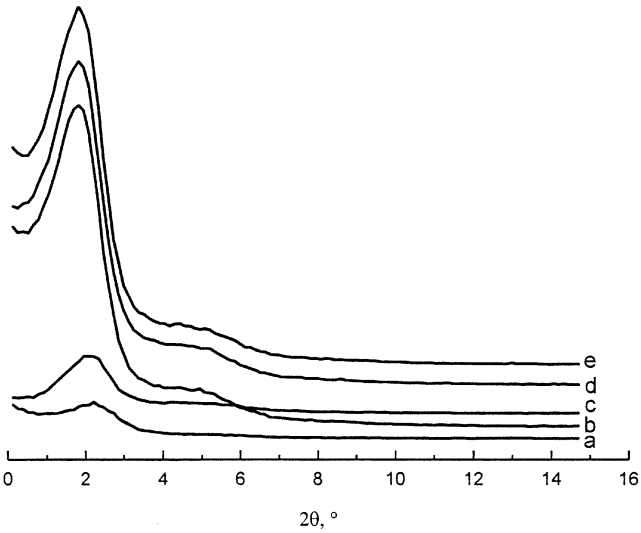

Figure 1. XRD patterns of siliceous MCM-41 and the proton-exchanged products. (a) Si–MCM-41, (b) H^+–MCM-41(8), (c) H^+–MCM-41(2), (d) H^+–MCM-41(4), (e) H^+–MCM-41(6).

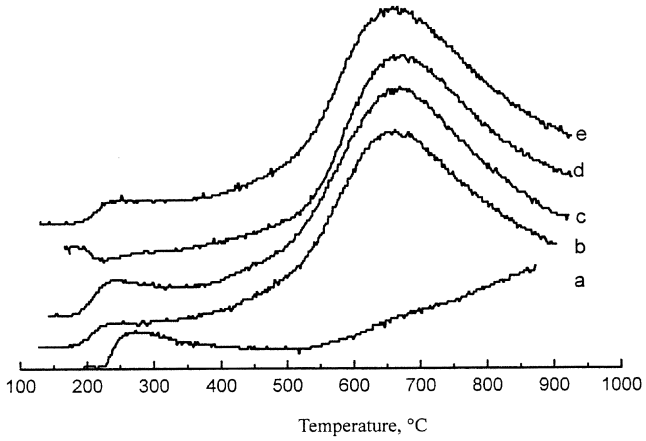

Figure 2. NH_3–TPD profiles of siliceous MCM-41 and the proton-exchanged products. (a) Si–MCM-41, (b) H^+–MCM-41(2), (c) H^+–MCM-41(4), (d) H^+–MCM-41(6), (e) H^+–MCM-41(8).

derived from C–C bond hydrogenolysis of BP and CHB; thus the selectivity of the total of benzene and cyclohexane (S_{B+C}) is used to evaluate the hydrocracking activity.

Figure 4 shows the variation of DBT conversion with temperature. It is indicated that Ni–Mo/H^+–MCM-41(t) showed higher activity than Ni–Mo/Si–MCM-41 in converting DBT into hydrocarbons, yielding almost complete conversion at temperatures over 320 °C. Both Ni–Mo/H^+–MCM-41(6) and Ni–Mo/H^+–MCM-41(8) exhibit the highest activities for DBT hydrodesulfurization. In contrast, the introduction of Na^+ to the MCM-41 matrix significantly decreases the catalytic activity of Ni–Mo/H^+–MCM-41(6), indicating that Na cations have negative effects on the HDS activity of the supported Ni–Mo catalysts.

The proton exchange of MCM-41 with HNO_3 also leads to a dramatic increase of the ratio of S_{CHB} to S_{BP}, as shown in figure 5. The higher S_{CHB}/S_{BP} implies that the proton-exchanged supports favor the formation of the hydrogenation active sites on the surface. On the contrary, the introduction of Na^+ to the support leads to the decrease of S_{CHB}/S_{BP}, suggesting that Na^+ is detrimental to the formation of the hydrogenation active sites and thus to the HDS activity. These results indicate that the HDS of DBT takes place mainly through hydrogenolysis for Ni–Mo/Si–MCM-41 and Ni–Mo/Na–MCM-41, whereas both hydrogenolysis and hydrogenation play important roles for H^+–MCM-41-supported Ni–Mo catalysts.

Earlier research [16] has shown that hydrogenation and hydrogenolysis occur on different kinds of catalytic sites. The different performance of Ni–Mo/H^+–MCM-41(6) and Ni–Mo/Na–MCM-41 suggests that Na cations contained in MCM-41 may hinder the formation of the hydrogenation sites, leading to the low hydrogenation activity of Ni–Mo/Na–MCM-41, and the higher hydrogenation activity of Ni–Mo/H^+–MCM-41 may be attributed to the removal of Na^+ by the proton exchange.

Figure 6 illustrates the variations of the S_{B+C} with temperature. It is shown that the S_{B+C} for Ni–Mo/H^+–MCM-41 increased with increasing temperature, while that for Ni–Mo/Si–MCM-41 and Ni–Mo/Na–MCM-41 decreased with increasing temperature. Among the Ni–Mo catalysts supported on the proton-exchanged MCM-41, Ni–Mo/H^+–MCM-41(8) exhibits the highest hydrocracking activity, increasing almost linearly with temperature in the temperature range investigated. The dramatic increase in the S_{B+C} of Ni–Mo/H^+–MCM-41 indicates that the hydrocracking activity of Ni–Mo/MCM-41 was enhanced by the proton exchange of MCM-41 with HNO_3. The increased hydrocracking activity may be attributed to the strong acid sites on the proton-exchanged MCM-41. Since the Na^+ in MCM-41 may kill the acid sites of the support, both Ni–Mo/Si–MCM-41 and Ni–Mo/Na–MCM-41 exhibit low hydrocracking activity.

The TPR profiles of MCM-41-supported Ni–Mo catalysts and Ni–Mo/γ-Al_2O_3 are illustrated in figure 7. Three TPR peaks were observed for Ni–Mo/γ-Al_2O_3, *i.e.*, low-temperature (LT) peak (470 °C), medium-temperature (MT) peak (590 °C) and high-temperature (HT) peak (720 °C). These peaks are in accordance with the Mo_I, Ni_I and $Mo_{II} + Ni_{II}$ peaks respectively, as described by Brito and Laine [17]. Generally, the LT peak is assigned to partial reduction of highly dispersed polymolybdate-like species (Mo_I), while the MT peak corresponds to a surface interaction compound (Ni_I) where Ni cations are all octahedrally coordinated [18]. Since the Mo_{II} and Ni_{II} peaks are completely superimposed, the HT peak is

Table 3
The surface acidity of Si–MCM-41 and the proton-exchanged products determined by the Hammett indicators.

Indicator (H_0)	Si–MCM-41	H^+–MCM-41(2)	H^+–MCM-41(4)	H^+–MCM-41(6)	H^+–MCM-41(8)
p-(Dimethylamino)azobenzene (+3.3)	+	+	+	+	+
Dicinnamalacetone (−3.0)	−	+	+	+	+
Benzalacetophenone (−5.6)	−	+	+	+	+
Anthraquinone (−8.2)	−	−	−	−	−

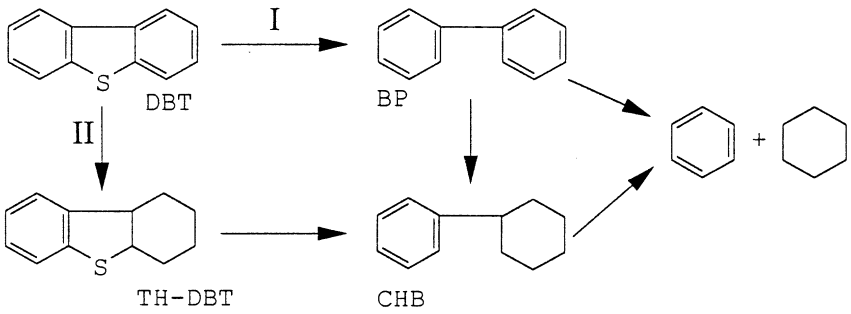

Figure 3. The reaction path network of DBT hydrodesulfurization.

assigned to the peak of ($Mo_{II} + Ni_{II}$). The Ni_{II} peak is identified with bulk-like $NiAl_2O_4$ [19], whereas the Mo_{II} peak is thought to be the composite of the subsequent reduction of such species plus the reduction of more

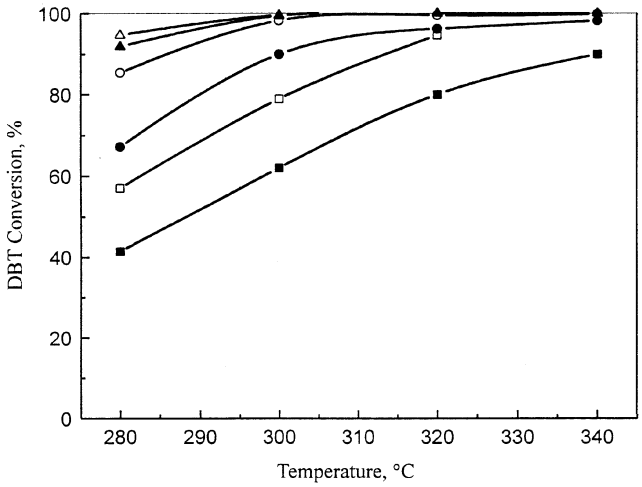

Figure 4. Variation of DBT conversion with temperature during HDS over the supported Ni–Mo catalysts. (□) Ni–Mo/Si–MCM-41, (●) Ni–Mo/H^+–MCM-41(2), (○) Ni–Mo/H^+–MCM-41(4), (△) Ni–Mo/H^+–MCM-41(6), (▲) Ni–Mo/H^+–MCM-41(8), (■) Ni–Mo/Na–MCM-41.

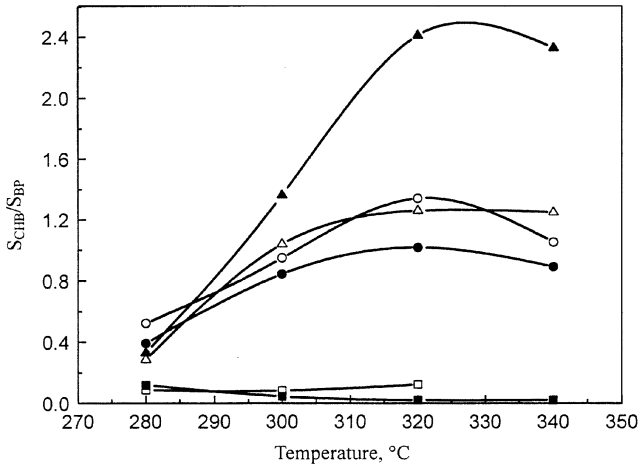

Figure 5. S_{CHB}/S_{BP} *versus* temperature during HDS of DBT over MCM-41-supported Ni–Mo catalysts. (□) Ni–Mo/Si–MCM-41, (●) Ni–Mo/H^+–MCM-41(2), (○) Ni–Mo/H^+–MCM-41(4), (△) Ni–Mo/H^+–MCM-41(6), (▲) Ni–Mo/H^+–MCM-41(8), (■) Ni–Mo/Na–MCM-41.

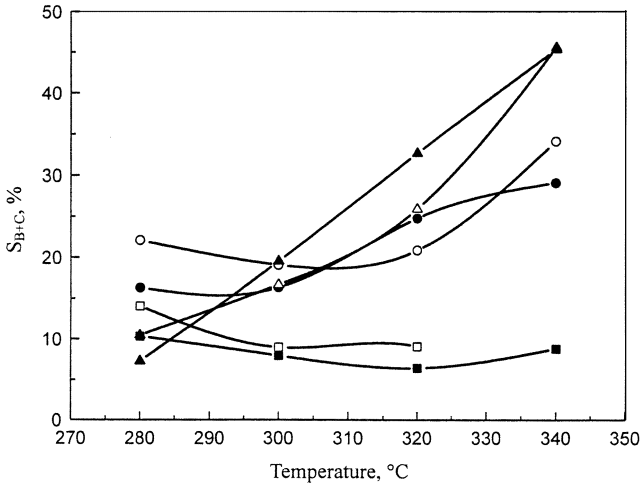

Figure 6. The variation of S_{B+C} with temperature during HDS of DBT. (□) Ni–Mo/Si–MCM-41, (●) Ni–Mo/H^+–MCM-41(2), (○) Ni–Mo/H^+–MCM-41(4), (△) Ni–Mo/H^+–MCM-41(6), (▲) Ni–Mo/H^+–MCM-41(8), (■) Ni–Mo/Na–MCM-41.

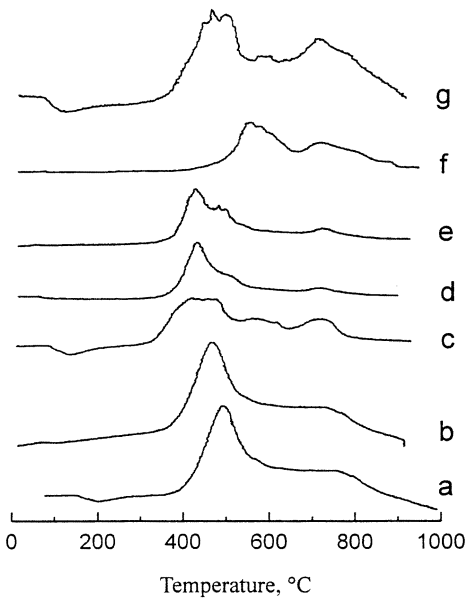

Figure 7. TPR profiles of the supported Ni–Mo catalysts. (a) Ni–Mo/Si–MCM-41, (b) Ni–Mo/H^+–MCM-41(2), (c) Ni–Mo/H^+–MCM-41(4), (d) Ni–Mo/H^+–MCM-41(6), (e) Ni–Mo/H^+–MCM-41(8), (f) Ni–Mo/Na–MCM-41, (g) Ni–Mo/γ-Al_2O_3.

Table 4
The main H_2 consumption temperatures in the TPR profiles of the supported Ni–Mo catalysts.

Catalyst	The LT peak temperature (°C)
Ni–Mo/Na–MCM-41	559
Ni–Mo/Si–MCM-41	493
Ni–Mo/H^+–MCM-41(2)	467
Ni–Mo/H^+–MCM-41(4)	447
Ni–Mo/H^+–MCM-41(6)	436
Ni–Mo/H^+–MCM-41(8)	428

refractory entities, including tetrahedrally coordinated molybdate groups [20,21]. It has been proposed that polarization effects of Al^{3+} ions may affect the covalence of the Mo–O bonds, and thus their reactivity toward hydrogen [22]. Accordingly, the less polarized bonds of polymolybdates are reduced more easily than those of the species directly tied to γ-Al_2O_3.

As for Ni–Mo catalysts supported over Si–MCM-41, only the LT peak was clearly observed. The disappearance or the decrease in intensity of the HT peak can be attributed to the decrease of the population of the more refractory species. It is assumed that the difference between Ni–Mo/MCM-41 and Ni–Mo/γ-Al_2O_3 may result from the high dispersion of the active species and the interactions between the active species and the supports. The main H_2 consumption temperatures of Ni–Mo/H^+–MCM-41(t) are summarized in table 4. The main consumption temperature Ni–Mo/H^+–MCM-41(t) decreases with the increase of the proton exchange time. It is shown that Ni–Mo/Na–MCM-41 showed the highest consumption temperature, indicating that this catalyst has lower reducibility. It is assumed that Na^+ is detrimental to the formation of hydrogenation active sites.

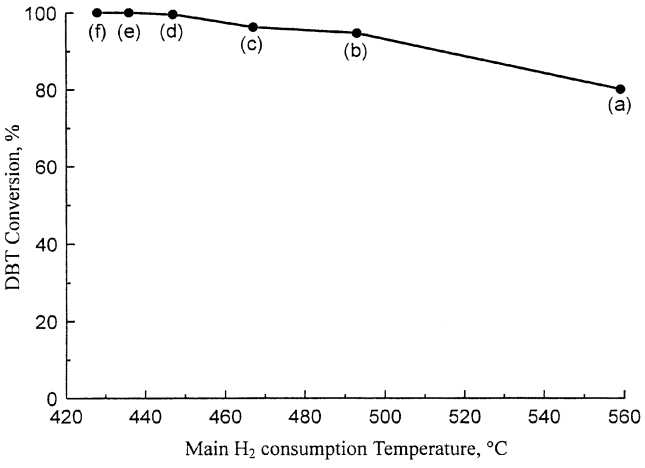

Figure 8. The DBT conversion at 320 °C *versus* main H_2 consumption temperatures in the TPR profiles of the MCM-41-supported Ni–Mo catalysts. (a) Ni–Mo/Na–MCM-41, (b) Ni–Mo/Si–MCM-41, (c) Ni–Mo/H^+–MCM-41(2), (d) Ni–Mo/H^+–MCM-41(4), (e) Ni–Mo/H^+–MCM-41(6), (f) Ni–Mo/H^+–MCM-41(8).

The DBT conversion at 320 °C is plotted against the main H_2 consumption temperature for the supported Ni–Mo catalysts, as shown in figure 8. It is indicated that DBT conversion is well correlated with the consumption temperature for the MCM-41-supported Ni–Mo catalysts.

4. Conclusions

It is observed that the mesostructure of siliceous MCM-41 was improved by ion exchange with dilute HNO_3 solutions. Most of the sodium cations contained in MCM-41 were removed by proton exchange, and dealuminization was observed during the ion exchange. New strong acid sites ($-5.6 > H_0 > -8.2$) were generated by the proton exchange, but the following proton exchange has little effect on the structural and acidic properties of siliceous MCM-41. It seems that HNO_3 clears the pore channels of MCM-41 during the ion exchange and reconstruction of the mesostructure may contribute to the increase of the crystallinity. Nevertheless, destruction of the structure of the mesoporous material was observed when the proton exchange time reached 8 h. The results of both NH_3–TPD and Hammett indicators indicate that strong acid sites might be generated after the proton exchange.

When Ni–Mo species were supported on the proton-exchanged MCM-41, great improvement in HDS activity was observed, and it is indicated that the improvement is accompanied by the increase of S_{CHB}/S_{BP}, suggesting that the proton-exchanged supports favor the formation of the hydrogenation active sites on the surface. On the contrary, the introduction of Na^+ into the matrix of the support leads to the decrease in both HDS activity and S_{CHB}/S_{BP}, indicating that Na^+ is detrimental to the formation of the hydrogenation active sites and thus to the HDS activity of DBT. The proton exchange of MCM-41 also leads to the increase in the hydrocracking activity of Ni–Mo/H^+–MCM-41(t). The higher hydrocracking activity may be attributed to the strong acid sites on the surface of H^+–MCM-41. The TPR results indicate that DBT conversion is well correlated with the main H_2 consumption temperature, suggesting that the HDS activity is improved by the enhanced reducibility of the catalysts.

Acknowledgments

This research was financially supported by the Natural Science Foundation of China (20003002) and by the Young Promising Teachers' Funds from the Education Ministry of China. The authors are grateful to Mr. D. Han, Ms. B. Zhao, Mr. Z. Sun and Mr. C. Li for their kind help in the research work.

References

[1] J.S. Beck, J.C. Vartuli, W.J. Routh, M.E. Leonowicz, C.T. Kresge, K.D. Schmitt, C.T.-W. Chu, D.H. Olson, E.W. Sheppard, S.B. McCullen, J.B. Higgins and J.L. Schlenker, J. Am. Chem. Soc. 114 (1992) 10834.

[2] A. Corma, V. Fornés, M.T. Navarro and J. Pérez-Pariente, J. Catal. 148 (1994) 569.

[3] J.Y. Ying. C.P. Mehnert and M.S. Wong, Angew. Chem. Int. Ed. 36 (1999) 56.

[4] A. Corma, A. Martínez, V. Martínez-Soria and J.B. Montón, J. Catal. 153 (1995) 25.

[5] K.M. Reddy, B. Wei and C.S. Song, Catal. Today 43 (1998) 261.

[6] C.S. Song and K.M. Reddy, Appl. Catal. A Gen. 176 (1999) 1.

[7] J. Ramírez, R. Contreras, P. Castillo, T. Klimova, R. Zárate and R. Luna, Appl. Catal. A Gen. 197 (2000) 69.

[8] T. Klimova, M. Calderón and J. Ramírez, in: *13th International Zeolite Conference*, Montpelier, France, 26 P12, 8–13 July 2001.

[9] V.R. Choudhary and S.D. Sansare, Proc. Ind. Acad. Sci. (Chem. Sci.) 109 (1997) 229.

[10] Z. Luan, H. He, W. Zhou, C.F. Cheng and J. Klinovski, J. Chem. Soc. Faraday Trans. 91 (1995) 2955.

[11] A. Wang, Y. Wang, T. Kabe, Y. Chen, A. Ishihara and W. Qian, J. Catal. 199 (2001) 19.

[12] A. Wang, X. Li, Y. Chen, D. Han, Y. Wang, Y. Hu and T. Kabe, Chem. Lett. (2001) 474.

[13] W. Qian, A. Ishihara, S. Ogawa and T. Kabe, J. Phys. Chem. 98 (1994) 907.

[14] A. Corma, Chem. Rev. 95 (1995) 559.

[15] A. Wang and T. Kabe, Chem. Comm. (1999) 2067.

[16] M.J. Girgis and B.C. Gates, Ind. Eng. Chem. Res. 30 (1991) 2021.

[17] J.L. Brito and J. Laine, J. Catal. 139 (1993) 540.

[18] B. Scheffer, P. Molhoek and J.A. Moulijn, Appl. Catal. 46 (1989) 11.

[19] P. Dufresne, E. Payen, J. Grimblot and J.P. Bonnele, J. Phys. Chem. 85 (1981) 2344.

[20] P. Arnoldy, M.C. Franke, B. Scheffer and J.A. Moulijn, J. Catal. 96 (1985) 381.

[21] J. Brito and J. Laine, Polyhedron 5 (1986) 179.

[22] P. Arnoldy and J.A. Moulijn, J. Catal. 93 (1985) 38.